



Photo-crosslinked gelatin-hyaluronic acid methacrylate hydrogel-committed nucleus pulposus-like differentiation of adipose stromal cells for intervertebral disc repair

Pengfei Chen[†] | Lei Ning[†] | Pengcheng Qiu[†] | Jian Mo | Sheng Mei | Chen Xia |
Jianfeng Zhang | Xianfeng Lin | Shunwu Fan

Department of Orthopaedics, Sir Run Run Shaw Hospital, School of Medicine, Zhejiang University, Hangzhou, China

Correspondence

Jianfeng Zhang, Xianfeng Lin, and Shunwu Fan, Department of Orthopaedics, Sir Run Run Shaw Hospital, School of Medicine, Zhejiang University, #3 Qing Chun Road, Hangzhou 310016, China.

Email: dr_zhangjianfeng@163.com; xianfeng_lin@zju.edu.cn; shunwu_fan@zju.edu.cn

Funding information

Key research and development plan in Zhejiang Province, Grant/Award Number: 2018C03060; Natural Science Fund of Zhejiang Province, Grant/Award Numbers: LY16H060004, LZ15H060002 and Y18H060001; National Nature Science Fund of China, Grant/Award Numbers: 81871797, 81772387, 81702143 and 81802147

Abstract

Nucleus pulposus-like differentiation is always the challenge with application of stem cells for intervertebral disc repair. The combination of injectable biomaterials and stem cells may provide a resolution for this problem, as the transmembrane force can affect the intracellular environment through integrin $\alpha\beta$. In this study, we developed a strategy of photo-crosslinked gelatin-hyaluronic acid methacrylate (GelHA) hydrogel to commit the nucleus pulposus-like differentiation of adipose stromal cells (ASCs) for intervertebral disc repair. ASCs were isolated and cultured in GelHA hydrogel to evaluate nucleus pulposus-like differentiation. The function of integrin $\alpha\beta\beta_6$ was investigated with neutralising antibody. The efficacy of ASCs with GelHA hydrogel for intervertebral disc repair was studied in a rat model of intervertebral disc degeneration. The results showed that GelHA hydrogel promoted ASCs nucleus pulposus-like differentiation and that integrin $\alpha\beta\beta_6$ neutralising antibody prevented ASCs from expression of nucleus pulposus matrix in vitro. The combination of GelHA hydrogel and ASCs promoted quality intervertebral disc repair in rats with much more nucleus pulposus matrix and significantly higher disc height index. The findings have demonstrated that the combination of photo-crosslinked GelHA hydrogel and ASCs can commit ASCs to nucleus pulposus-like differentiation and improve the efficacy of ASCs for intervertebral disc repair. These findings suggest a promising stem cell-based strategy for intervertebral disc repair.

KEYWORDS

adipose stem cells, cellular proliferation, hydrogel, integrins, intervertebral disc, microenvironment

1 | INTRODUCTION

Intervertebral disc degeneration (IVDD) is a global health problem that has caused serious social and economic consequences (Carlesso, Raja Rampersaud, & Davis, 2017). In the United States, the total cost of low back pain caused by IVDD is about 1.5% of the gross domestic

product (Patrick, Emanski, & Knaub, 2014). Conservative treatment and surgery are the primary approaches at present. However, the function of the disc cannot be re-established through these ways (May, 2013).

The intervertebral disc is a special organ composed of a nucleus pulposus (NP), an annulus fibrosus (AF), and two cartilage endplates

[†]Authors contributed equally to this work.

that connect adjacent vertebrae (Colombier, Clouet, Hamel, Lescaudron, & Guicheux, 2014). The NP is the central part of the intervertebral disc. Previous study has elucidated the phenotype of NP cells, including PAX1, OVOS2, CD24, CA12, ACAN, and COL2A1 markers (Minogue, Richardson, Zeef, Freemont, & Hoyland, 2010). Also, studies have identified relevant markers for NP cells in rats, including GLUT-1, MMP-2, GPC3, and K19 (Anderson et al., 2005; Yang & Li, 2009). NP cells play a vital role in producing the NP extracellular matrix (ECM). The decrease in the activity of NP cells is one of the major causes leading to irreversible degeneration of the NP and the complete loss of biomechanical properties of the intervertebral disc.

In early- or middle-stage IVDD, replenishing stem cells into the NP may be a promising method to reconstruct the functions of the intervertebral disc (Chaofeng et al., 2013). Bone marrow mesenchymal stem cells (BMSCs) and adipose stromal cells (ASCs) were the most common cells used for study. One study showed that BMSCs have the ability to differentiate into NP-like cells (Steck et al., 2005). Meanwhile, ASCs also had this potential for NP-like cell differentiation (Clarke et al., 2014; Minogue et al., 2010). However, the problem of the multidirectional differentiation of stem cells still exists when applied to intervertebral disc. A study reported that the injection of stem cells into NP may lead to the formation of osteophytes, which aggravated the degeneration of intervertebral disc (Vadala et al., 2012). Therefore, it is of great importance to develop a program that can differentiate stem cells into NP-like cells with the same phenotype and biological activity.

The combination of injectable biomaterials and stem cells may provide a resolution for this problem. Research found that ASCs cultured in alginate hydrogels showed an increase of cartilage-related gene expression (Zeng et al., 2015). Our previous studies also found that photo-crosslinked gelatin methacrylate (GelMA) hydrogels can promote the expression of articular cartilage ECM (Chen et al., 2016). However, the mechanical properties of the GelMA hydrogel cannot reach the natural level of the NP. The addition of hyaluronic acid methacrylate (HAMA) may help to increase its mechanical properties (Camci-Unal, Cuttica, Annabi, Demarchi, & Khademhosseini, 2013).

It has been known that the physical properties of biomaterials, such as mechanical stiffness, permeability, and microenvironment, can regulate the reprogramming and differentiation of stem cells (Downing et al., 2013). A study reported that transmembrane force can affect the intracellular environment through integrin $\alpha\beta$ (Dong et al., 2017). Integrin is a heterodimer consisting of alpha and beta subunits (Ye, Lagarrigue, & Ginsberg, 2014). Integrin $\alpha\beta_6$ can transfer mechanical stimulation between the extracellular ligand and the actin cytoskeleton. Integrin $\alpha\beta_6$ binds to the predomain, exerts a force, and releases transforming growth factor beta (TGF- β) growth factor in the activation of transforming growth factor beta 1 (TGF- β_1) precursors. And TGF- β_1 plays an important role in the development of intervertebral discs (Baffi et al., 2004). One study has reported that the intervertebral disc (IVD) was greatly reduced or missing in the axial skeleton of mice in which TGF- β Type 2 receptor (Tgf- β RII) was deleted in Col2a-expressing cells. Also,

Tgf- β RII was required to maintain the boundary between the vertebrae and IVD (Baffi, Moran, & Serra, 2006). However, there is no research about how integrin promote the NP-like differentiation.

In this paper, the combination of photo-crosslinked gelatin-hyaluronic acid methacrylate (GelHA) hydrogel and ASCs was used to reconstruct the intervertebral disc. First, the crosslinking GelHA hydrogel was prepared and the tissue-engineered NP was constructed in vitro. Second, we explored the role of GelHA hydrogel in the proliferation and differentiation of ASCs in vitro. We also determined how the hydrogel affect the integrin $\alpha\beta_6$ -TGF- β pathway through mechanical stimulus as well as the possible mechanism of NP-like differentiation. Finally, rat model was used to evaluate the efficacy of optimised GelHA hydrogel and ASCs in repairing IVDD.

2 | MATERIALS AND METHODS

2.1 | Materials

Gelatin (Type A, 300 bloom from porcine skin) and methacrylic anhydride (MA) were purchased from Sigma-Aldrich (St. Louis, Missouri). Sodium hyaluronate (Molecular weight: 403.3) was purchased from Aladdin Chemistry Co., Ltd. (Shanghai, China). All other chemicals were purchased from Sigma-Aldrich unless specifically mentioned.

2.2 | Synthesis of polymer precursors

GelMA was synthesised according to a procedure described previously (Chen et al., 2016). Briefly, gelatin was mixed into phosphate-buffered saline (PBS) at a concentration of 10% (w/v). MA was added to the gelatin solution and allowed to react for 1 hr. Following a 5 \times dilution PBS to stop the reaction, the mixture was dialyzed for 1 week. The solution was lyophilised for 1 week and stored at -80°C . The degree of methacrylation was determined as $\sim 78\%$ by ^1H NMR (Figure S1). HAMA was also synthesised following a previously described procedure (Burdick, Chung, Jia, Randolph, & Langer, 2005). Briefly, 1 g hyaluronic acid sodium salt was dissolved in 100 mL distilled water. MA was then added to this solution and the reaction was performed for 24 hr. The resulting solution was dialyzed for 3 days and lyophilised, which was then kept at -80°C until further use. The methacrylation degree was measured as $\sim 25\%$ by ^1H NMR (Figure S1). The prepolymer hydrogel solution was prepared by mixing 5 wt% GelMA solution and 1 wt% HAMA into PBS containing 0.5% (w/v) 2-hydroxy-1-(4-(hydroxyethoxy)phenyl)-2-methyl-1-propanone (Irgacure 2959, CIBA Chemicals, Basel, Switzerland) as a photoinitiator at 80°C . The prepolymer solution was vigorously stirred at room temperature for 10 min to generate a homogeneous solution, which was pipetted into a 24-well culture dish (200 μL /well) and exposed to ultraviolet (UV) light (365 nm, 7.0 mW/cm 2) for 2 min to allow for photo-crosslinking. The samples were incubated in a free-floating manner at 37°C in PBS for 24 hr, followed by storage at -20°C .

2.3 | Mechanical testing

After UV crosslinking, the hydrogels were rinsed with PBS and further maintained in PBS for 24 hr. The hydrogels were punched using a 5-mm biopsy punch prior to mechanical testing. The excess liquid from the hydrogel discs was removed using Kimwipes. Compression testing was carried out by applying a strain rate of 0.2 mm/min using an Instron testing machine (Model 5543; Instron, Canton, Massachusetts) and software (Bluehill V2.0; Instron). We determined the compressive modulus by taking the slope in the linear section of the stress-strain curve at 5%–10% strain area. Five replicates were used for each group.

2.4 | Scanning electron microscopy characterisation

To characterise the internal microstructures of the materials, the samples were frozen at -80°C and lyophilised. The dried samples were mounted on aluminium stubs, sputter-coated with gold, and observed under a scanning electron microscope (Hitachi S3000 N) at an accelerating voltage of 15 kV.

2.5 | Isolation of rat ASCs and NP cells

Rat ASCs were isolated from the inguinal area of 6-week-old male Sprague–Dawley rats weighing 160 ± 5 g, as described previously (Zhu et al., 2014). The cells were cultured in Dulbecco's modified Eagle's medium (DMEM) supplemented with 10% foetal bovine serum (Gibco, Grand Island, New York, <http://www.invitrogen.com>). The fourth to sixth passage cells were used for the experiments. Cultured cells were in monolayers on tissue culture polystyrene at 10^3 cells/cm² (ASCs group) or in GelHA hydrogels (GelHA + ASCs group). For cells in hydrogels, they were detached from tissue culture plate and mixed with prepolymer hydrogel solution at a final concentration of 5×10^6 cells/ml supplemented with 10% FBS (Invitrogen). Then the mixture was photo-crosslinked and used for further investigation. To promote ASCs differentiation, the cells were cultured in DMEM supplemented with 50 mg/ml ascorbic acid (Sigma-Aldrich), 10 mM of β -glycerol phosphate (Sigma-Aldrich), and 1 mM of dexamethasone (Sigma-Aldrich). The ASCs cultured in DMEM without supplements were regarded as the control group. For integrin $\alpha\beta6$ -TGF- β 1 pathway blocking, neutralising antibody of integrin $\alpha\beta6$ (10D5, 100 $\mu\text{g}/\text{ml}$) was added into the medium.

NP tissues were macroscopically isolated from the lumbar IVD of 4-week-old male Sprague–Dawley rats. Next, the tissues were diced into small pieces and treated with 0.025% collagenase II (Roche Diagnosis, Tokyo, Japan) at 37°C for 4 hr. NP cells were cultured in DMEM supplemented with 10% foetal bovine serum in a humidified incubator containing 5% CO₂. Second-passage cells were used in the following experiments.

2.6 | Cell viability detection

Live and dead assay was used to observe the cell status in GelHA hydrogel by fluorescence microscope (Nikon Eclipse Ti-S). Calcein-AM (2 μM , Dojindo) and Propidium Iodide (10 $\mu\text{g}/\text{ml}$) were used to dye live cells and dead cells, respectively. All these experiments were repeated three times.

2.7 | Quantitative reverse transcription polymerase chain reaction

Total RNA was extracted from mashed hydrogel using Trizol reagent (Invitrogen) following the manufacturer's instructions. The cDNA was reversely transcribed with Moloney Murine Leukemia Virus (MMLV) reverse transcription reagents (Takara). Glyceraldehyde 3-phosphate dehydrogenase were applied as normalisation control. Real-time PCR was done using SYBR premix qPCR kit (Takara). The primers being used were listed in Table 1. All experiments were performed in triplicate on three separate occasions.

2.8 | Rat IVDD model and animal experiments

Sprague–Dawley rats, aged at 12-weeks, weighing approximately 200 g, were used in this study ($n = 16$). All rats were treated according to the standard guidelines approved by the Zhejiang University Ethics Committee. Animals were anaesthetised with a combination of ketamine and xylazine (10:7, 100 mg/kg injected intraperitoneally).

The coccygeal intervertebral spaces Co5–6, Co6–7, Co7–8, and Co8–9 were selected for the study and were performed with the needle puncture. The selected coccygeal intervertebral levels were identified by digital palpation and confirmed by fluoroscopy. After tail skin antisepsis with alcohol iodate and using fluoroscopy, a 20-gauge needle was inserted at the level of the AF, crossing the NP up to the contralateral AF. After full penetration, the needle was rotated 360° twice and held for 30 s. The depth of needle penetration was controlled by the resistance of the contralateral AF.

4 weeks after initial operation, the selected coccygeal intervertebral levels were identified by digital palpation and confirmed by fluoroscopy. Then, the injured disc Co 5–6 remained no treatment as a degenerated sham group. Co6–7 was injected with 10 μl of 1×10^5 ASCs (ASCs group). Co7–8 was transplanted with 10 μl GelHA without cells (GelHA group). Co8–9 was injected with 10 μl GelHA with 1×10^5 ASCs (GelHA + ASCs group). In all animals, intact disc Co9–10 was served as noninjured control (NC group). For injection, 10 μl GelHA, with or without ASCs, was placed in a microsyringe with a 33-gauge needle (Hamilton 1700; Hamilton, Switzerland). After 2 min of photo-crosslinking, the hydrogel was injected into the intervertebral disc of the rat. Observation points included 0, 4, 8, and 12 weeks post treatments. The changes in coccygeal discs were assessed using radiographs, magnetic resonance imaging, and histological staining of NP tissue.

TABLE 1 Primer sequences for QRT-PCR

| Gene | Sense | Antisense |
|---------------|--|--|
| <i>Col2a1</i> | 5'-AGTCGCTGGTGTCTGCTGAC-3' | 5'-GGGGTCCTTTAGGTCTACG-3' |
| <i>ACAN</i> | 5'-CTGCTACACAGGTGAAGACTTTGTAGACATCC-3' | 5'-TGCTGTGCCTCCTCAAATGTCAGAGAGTATCT-3' |
| <i>CD24</i> | 5'-GGACATGGGCAGAGCGAT-3' | 5'-TTTCTTGGCCTGAGTCTCTAACAGT-3' |
| <i>PAX1</i> | 5'-TGGCCCTCGGCTCATT-3' | 5'-GCCCCTGTTTGTCCATAAA-3' |
| <i>OVOS2</i> | 5'-CCTCCAAGCAGGGAGTTTTG-3' | 5'-TATCCCCACAACAGTGAAAAAG-3' |
| <i>GLUT-1</i> | 5'-TCTCTGGGTAAACAGGGATCAAACA-3' | 5'-ACTGCAACGGCTTTAGACTTCGAC-3' |
| <i>MMP-2</i> | 5'-GGCCCTGTCACTCCTGAGAT-3' | 5'-GGCATCCAGTTATCGGGGA-3' |
| <i>GPC3</i> | 5'-GGCCCTGAGCCAGTGGTT-3' | 5'-TTTACCCTTGGGCACAGACAT-3' |
| <i>K19</i> | 5'-CCAGGACCCAGCTGGAGAT-3' | 5'-ACTAATTTCTCCTCGTGGTTCTTC-3' |
| <i>GAPDH</i> | 5'-ATCACTGCCACCCAGAAGAC-3' | 5'-ATGAGGTCCACCACCTGTT-3' |

Note. QRT-PCR: quantitative reverse transcription polymerase chain reaction.

2.9 | Histological analysis and immunohistochemistry of IVD motion segments

Sample of IVD motion segments from in vivo studies were fixed in cold 10% neutral-buffered formalin for 1 week. Then, the samples were immersed into the decalcifying liquid (14% EDTA) for 6 weeks, shaking gently at room temperature. Decalcifying liquid was changed every 2 days. Subsequently, the samples were dehydrated in an alcohol gradient, cleared, and embedded in paraffin blocks. Histological sections (8 μ m) were prepared using a microtome. Six representative sections of each sample from various depths were mounted on slides, stained with safranin-O, and photographed digitally under a microscope.

Sections evaluated by immunofluorescence were blocked by incubation with 5% (w/v) BSA, incubated with primary antibodies for $\alpha\beta6$, COL2A1 and aggrecan, incubated with corresponding secondary antibodies conjugated to AlexaFluor 488 fluorescent dye (Invitrogen), and stained with DAPI (Beyotime Institute of Biotechnology). After staining, the histological sections were viewed under a microscope. The number of positively stained cells on the NP was counted in five sequential sections per sample in each group.

2.10 | Statistical analysis

All quantitative data are presented as mean \pm SD. Statistical data were analysed using one-way analysis of variance/Tukey's post-hoc test. For all experiments, $p < 0.05$ was considered to be significant and is indicated by *. $P < 0.01$ is indicated by **.

3 | RESULTS

3.1 | Preparation and characterisation of GelHA hydrogels

The GelHA hydrogel was fabricated by UV-induced crosslinking in the presence of a photoinitiator (Figure 1a). Figure 1b showed the

gelation of the hydrogel after UV crosslinking. We can see from the electron micrographs that the hydrogel had uniformly distributed pores (50–100 μ m, Figure 1c). Our previously study showed that photo-crosslinked GelMA hydrogel can promote expression of articular cartilage ECM. In the previous study, a 5% GelMA gel with a compressive modulus of 7.32 ± 0.61 kPa was used (Chen et al., 2016). In this study, the compressive moduli for hybrid hydrogels were found to be mechanically tunable by mixing HAMA and GelMA hydrogels at different concentrations (Figure 1d, Figure S2). Amongst them, we found that by adding 1% HAMA to 5% GelMA gel, its compressive modulus can be increased to 13.44 ± 0.60 kPa, which was similar to normal NP (13.44 ± 2.70 kPa) as reported (Zeng et al., 2015; Figure 1d). As the physical properties of biological materials might regulate the differentiation of stem cells, this optimised hydrogel was utilised for further evaluation.

3.2 | Biological characteristics of ASCs-laden GelHA hydrogels

To evaluate whether GelHA hydrogel could provide ASCs with an appropriate microenvironment for NP-like cell differentiation, the cell growth and multiple gene expression of ASCs cultured in the hydrogel were evaluated. Live and dead staining revealed that a large sum of live cells was observed after the GelHA culture of different time points (Figure 2a). Compared with the control group without supplements, the expressions of stem cell-related genes (OCT4, SOX2, and Nanog) in the ASCs group were significantly reduced ($p < 0.05$, Figure 2b). These genes in the GelHA + ASCs group were significantly down-regulated compared with the ASCs group ($p < 0.05$, Figure 2b). Moreover, the marker genes of NP cells in the GelHA + ASCs group were significantly up-regulated compared with the ASCs group and control group ($p < 0.01$, Figure 2c). Compared with the control group, only some marker genes (PAX1, COL2A1, ACAN, and MMP2) were up-regulated in the ASCs group ($p < 0.01$, Figure 2c). Similarly, immunofluorescence staining showed that the expressions of ACAN and COL2A1 in the GelHA + ASCs group were increased (Figure 3a–c).

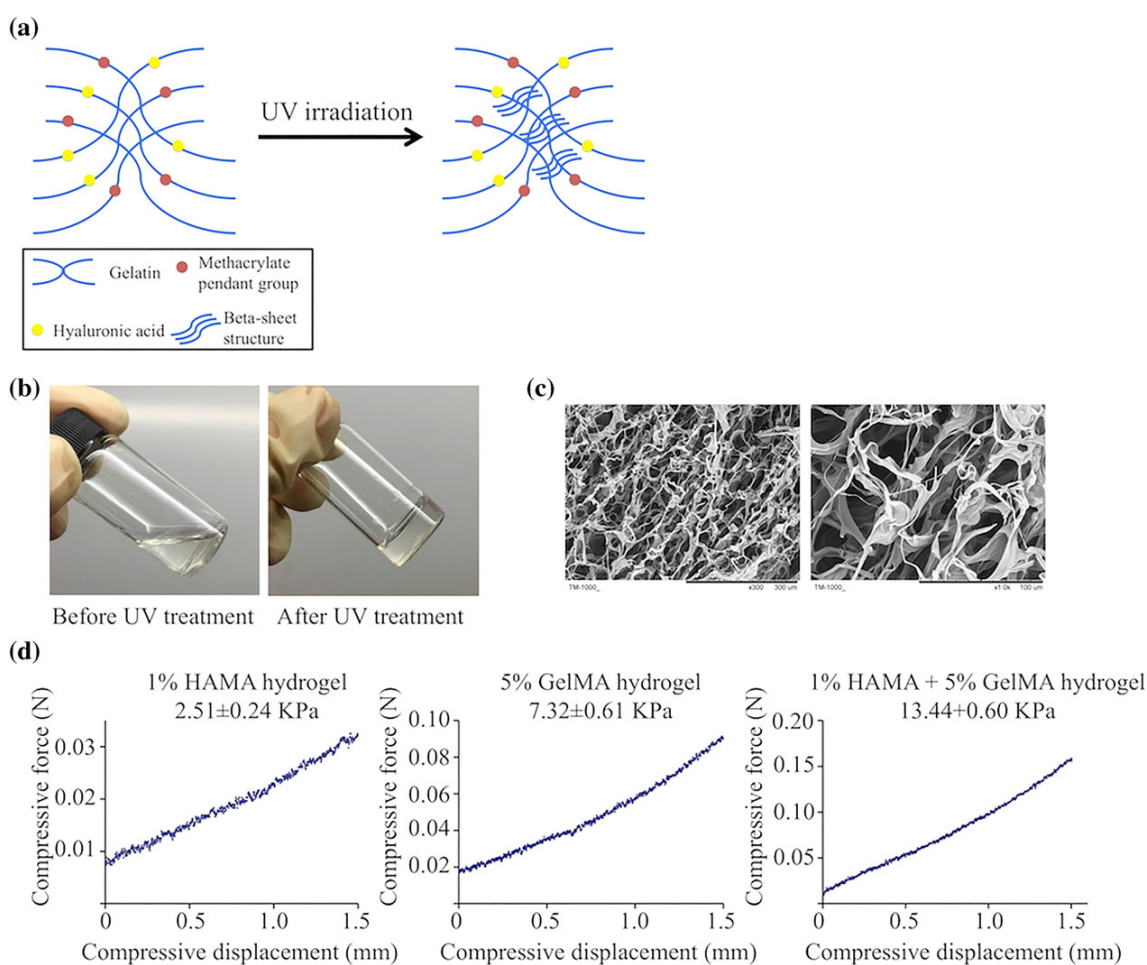


FIGURE 1 Preparation and characterisation of gelatin-hyaluronic acid methacrylate (GelHA) hydrogels. (a) Molecule structures and synthesis of polymer precursors of GelHA hydrogels. (b) GelHA hydrogels can be formed by ultraviolet (UV) irradiation for 1 min (left, before irradiation; right, after irradiation). (c) Microscopic structure of the hydrogels (low and high magnification). (d) The compressive moduli for the hydrogels, GelMA, gelatin methacrylate; HAMA, hyaluronic acid methacrylate [Colour figure can be viewed at wileyonlinelibrary.com]

Safranin O staining revealed that glycosaminoglycan deposition of the GelHA + ASCs group was also increased although compared with the control group (Figure 3d). After a 21-day culture, ASCs in the GelHA group exhibited similar morphology to the normal NP cells as shown in scanning electron microscope images (Figure 3e). Our results suggested that GelHA might provide ASCs with an appropriate microenvironment to differentiate into NP-like cells.

3.3 | Mechanisms in the NP-like differentiation of ASCs

We further explored the possible mechanisms in ASCs differentiation. Previous study had shown that TGF- β 1 could synergistically drive the NP-like differentiation process. As shown in Figure 4a, TGF- β 1 and TGF- β RII genes were all up-regulated in GelHA + ASCs group after 14- and 21-day culture as compared with normal cultured cells. Study reported that in activation of the TGF- β 1 precursor (pro-TGF- β 1), integrin bind to the prodomain, apply force, and release the TGF- β

growth factor (Dong et al., 2017). After 21-day culture, the expression of integrin α v β 6 was significantly elevated in GelHA + ASCs group compared with the control group (Figure 4b, Figure S3). Further, by utilising the neutralising antibody of integrin α v β 6 (10D5, 100ug/ml), the up-regulation of NP cell marker genes was significantly retarded ($p < 0.01$, Figure 4c). These results suggested that the GelHA hydrogel might promote the NP-like differentiation of ASCs by activating the integrin α v β 6- TGF- β 1 pathway.

3.4 | In vivo application of GelHA-ASCs to alleviate IVDD

Next, GelHA-ASCs were utilised in rat IVDD model. We evaluated the disc space by X-ray images and disc height index analysis (Figure 5a,b). Four weeks after operation, the disc space observed in all other groups was narrower than the NC group. Also, we found the disc height in the experimental groups continued to decline during the whole experimental period. However, disc height in ASCs

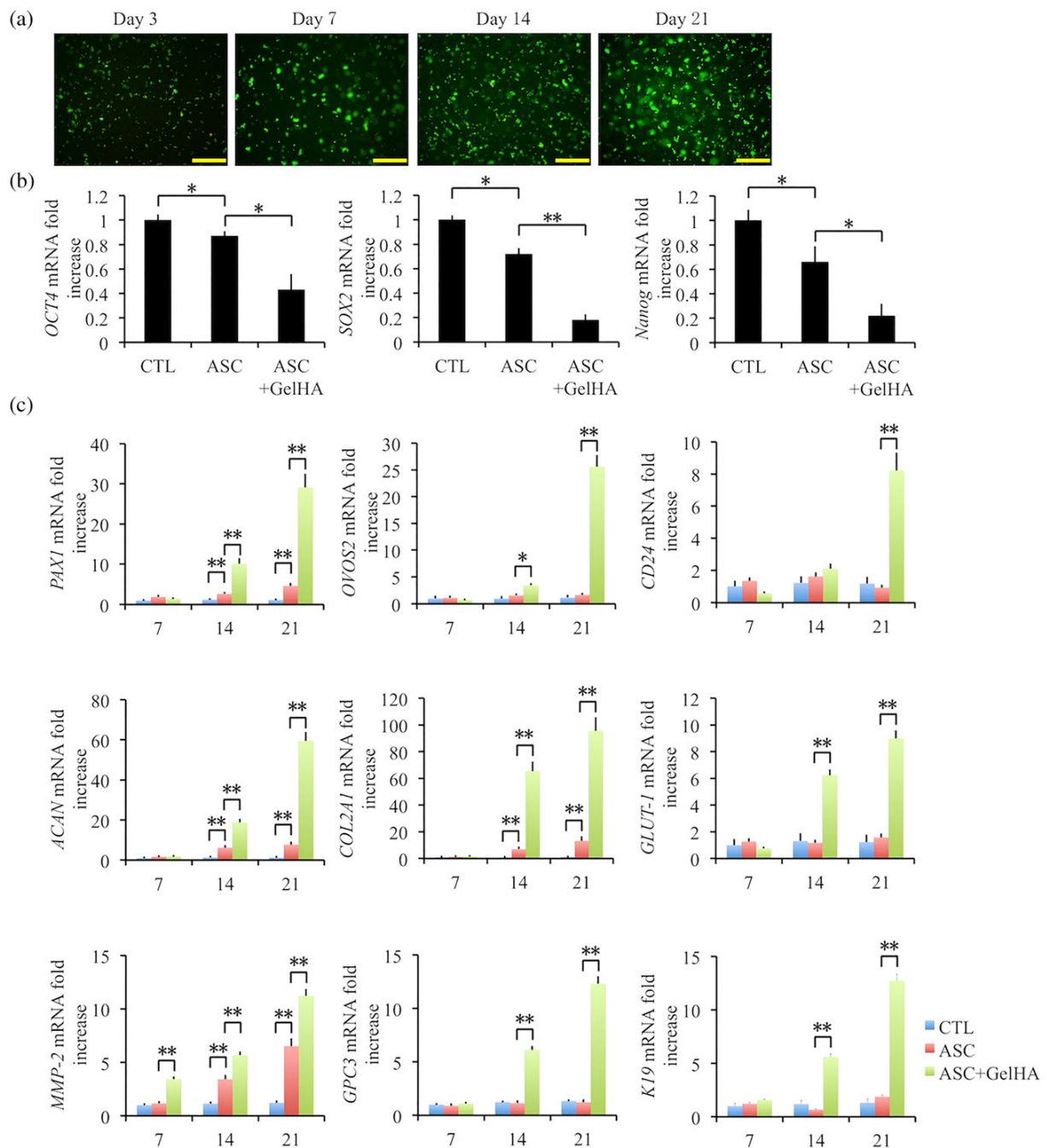


FIGURE 2 Biological characteristics of adipose stromal cells (ASCs)-laden gelatin-hyaluronic acid methacrylate (GelHA) hydrogels. (a) Live-dead cell staining of the ASCs cultured in GelHA hydrogels, scale bars = 200 μ m. (b) Expressions of stemness genes *OCT4*, *SOX2* and *Nanog* of ASCs were downregulated in GelHA hydrogels at Day 2 of culture. The gene expressed at Day 2 in ASCs cultured without supplements was used as a control. (c) The expression of *ACAN*, *COL2A1*, *CD24*, *OVOS2*, *PAX1*, *GLUT-1*, *MMP-2*, *GPC3*, and *K19* was analysed by reverse transcriptase quantitative polymerase chain reaction at 7, 14, and 21 days of culture. The gene expressed at Day 7 in ASCs cultured without supplements was used as a control. $n = 3$ (biological replicates), * $p < 0.05$, ** $p < 0.01$ (one way analysis of variance) [Colour figure can be viewed at wileyonlinelibrary.com]

group and GelHA group were significantly higher than the sham group in all time points. disc height index in GelHA + ASCs group declined slower than other treated groups at 4, 8, and 12 weeks. Throughout the study, mean signal intensity (SI) in NP tissue in NC

group did not change (Figure 5c,d). Compared with NC group, the mean SI in all treated groups was significantly lower after the initial operation. The mean SI in GelHA + ASCs group was significantly higher than other treated groups 4, 8, and 12 weeks. There was

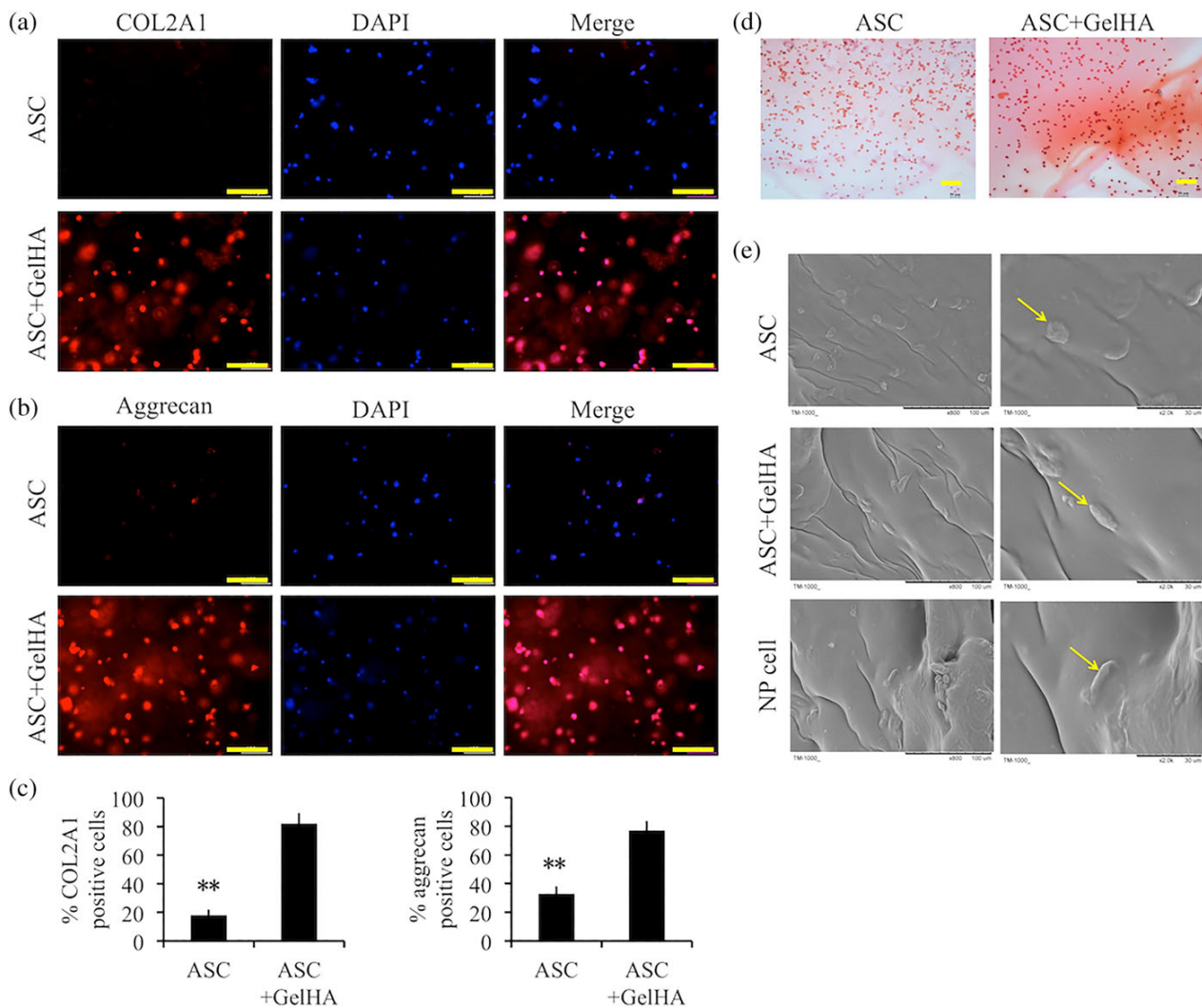


FIGURE 3 Evaluation of adipose stromal cells (ASCs) differentiation in gelatin-hyaluronic acid methacrylate (GelHA) hydrogels. (a and b) Immunofluorescence images showing the secretion of nucleus pulposus-related extracellular matrix at Day 21, scale bars = 200 μm . (c) Quantification of the COL2A1 and Aggrecan content. $n = 3$ (biological replicates), $**p < 0.01$ (one way analysis of variance). (d) Safranin O staining of GelHA hydrogels showing the glycosaminoglycan deposition at Day 21, scale bars = 200 μm . (e) Scanning electron microscope micrographs of ASCs and normal nucleus pulposus cells [Colour figure can be viewed at wileyonlinelibrary.com]

no significant difference between ASCs group and GelHA group, but the mean SI in these two groups was significantly higher than the sham group.

Twelve weeks after treatment, discs were collected for histological evaluation (Figure 6a). Discs from sham group exhibited severe degenerated NP tissues with narrowing discs. Although in NC group, intact NP tissues without narrowing discs can be observed. All other treated groups showed moderately degenerated NP tissues, whereas the narrowing disc spaces were restored. Amongst these groups, GelHA + ASCs group exhibited most satisfying results on NP tissues regeneration and disc spaces restoration. The results in GelHA group were similar with ASCs group. The GelHA hydrogel was degraded and cannot be found at 12 weeks.

Expression levels of ACAN and COL2A1 in NP tissues were compared amongst all groups by immunofluorescence (Figure 6b). Generally speaking, the results in GelHA + ASCs group were the most satisfying amongst all treated groups. Compared with ASCs group and GelHA group, expressions of ACAN and COL2A1 were significantly up-regulated in GelHA + ASCs group. Compared with sham group, expressions of ACAN and COL2A1 in ASCs group and GelHA group were significantly elevated. Further, we compared the expression levels of integrin $\alpha\beta6$ between GelHA + ASCs group and ASCs group. Both GelHA and GelHA + ASCs groups significantly increased the protein levels of integrin $\alpha\beta6$ compared with ASCs group, suggesting the GelHA hydrogel might activate the integrin $\alpha\beta6$ in vivo.

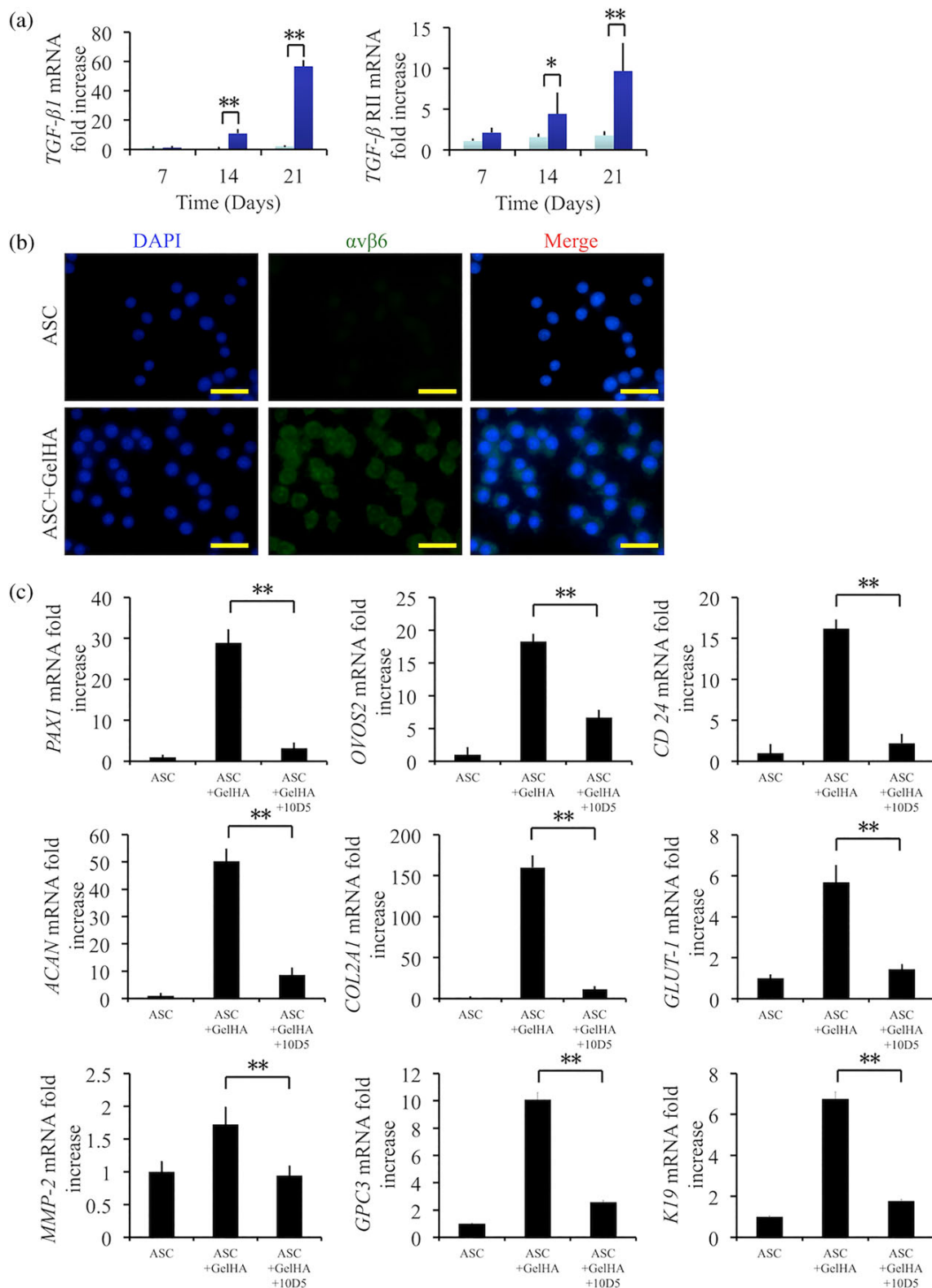


FIGURE 4 Mechanisms in the nucleus pulposus -like differentiation of adipose stromal cells (ASCs). (a) Transforming growth factor beta 1 (TGF-β1) and TGF-β Type 2 receptor (TGF-β RII) gene expression of ASCs seeded in gelatin-hyaluronic acid methacrylate (GelHA) hydrogels at Days 1, 14, and 21. (b) Immuno-staining of integrin $\alpha v \beta 6$ in ASCs after 21-day culture, scale bars = 100 μm . (c) The gene expression of ACAN, COL2A1, CD24, OVOS2, PAX1, GLUT-1, MMP-2, GPC3, and K19 was analysed after using the neutralising antibody of integrin $\alpha v \beta 6$. $n = 3$ (biological replicates), * $p < 0.05$, ** $p < 0.01$ (one way analysis of variance) [Colour figure can be viewed at wileyonlinelibrary.com]

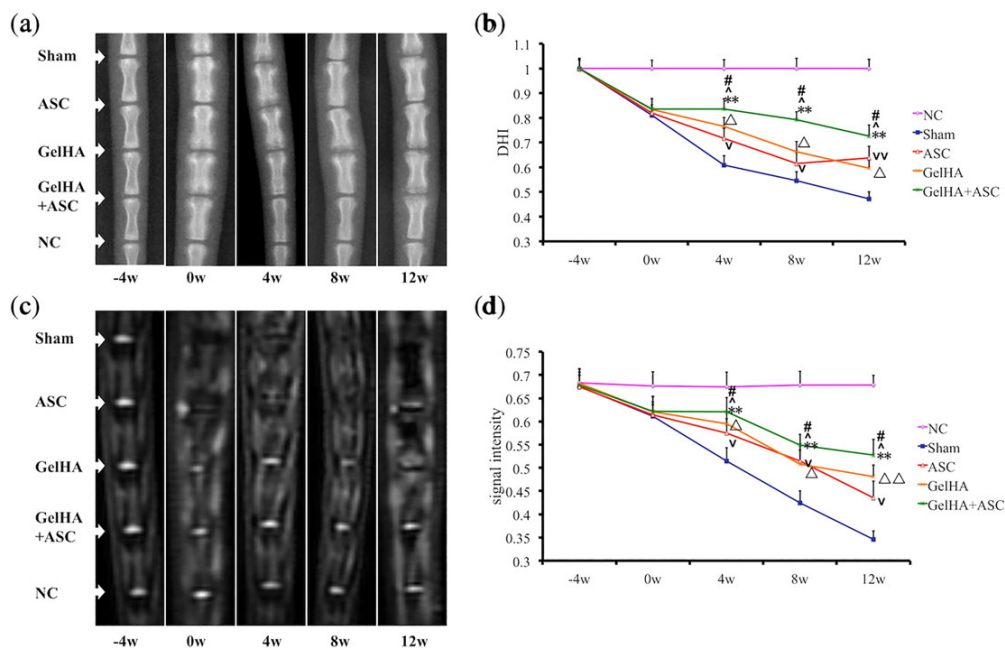


FIGURE 5 In vivo application of gelatin-hyaluronic acid methacrylate (GelHA)-adipose stromal cells (ASCs) to alleviate intervertebral disc degeneration. (a and c) Representative X-ray and magnetic resonance imaging images of the discs at -4, 0, 4, 8, and 12 weeks from different groups, including injection groups of free cells (ASCs, Co6–7), GelHA without cells (GelHA, Co7–8), and GelHA with ASCs (GelHA+ASCs, Co8–9). Degeneration group (sham, Co5–6) and intact group (noninjured control group, Co9–10) were taken as positive and negative control. (b and d) Disc height index (DHI) and T2-weighted signal intensity in different groups at 4, 8, and 12 weeks after the treatment. $n = 12$ (biological replicates). “#,” “^,” and “*” refers to GelHA + ASCs group compared with GelHA group, ASCs group, and sham group, respectively; “ Δ ” refers to ASCs group compared with sham group, “v” refers to GelHA group compared with sham group. #, ^, *, Δ , v = $p < 0.05$, ##, ^^, **, $\Delta\Delta$, vv = $p < 0.01$ (one way analysis of variance) [Colour figure can be viewed at wileyonlinelibrary.com]

3.5 | Summary of the therapeutic mechanism

In Figure S4, we speculated the therapeutic mechanism of GelHA + ASCs. The mechanical stress from hydrogels activated TGF- β 1 via the integrin $\alpha\beta$ 6. Activation of TGF- β 1 led to the enhancement of NP-like differentiation of ASCs and ECM (ACAN and COL2A1) secretion.

4 | DISCUSSION

In this study, we developed a new stem cell-based strategy for IVDD repair, in which photo-crosslinked GelHA hydrogel and ASCs were applied. Our study had several major findings. First, by adjusting the ratio of hydrogel, the compressive modulus of the hydrogel can be modified similar to normal NP. Second, this hydrogel committed the ASCs to NP-like differentiation by effectively regulating the integrin $\alpha\beta$ 6- TGF- β 1 pathway. Finally, the strategy of application GelHA hydrogel and ASCs improved the efficacy of ASCs for IVDD healing in rat model. These data suggest that the combination of GelHA hydrogel and ASCs can commit ASCs to NP-like differentiation and improve the efficacy of ASCs for IVD repair.

The present study has shown that ASCs cultured in GelHA hydrogel can differentiate into NP-like cells. ASCs could be an alternative autologous cell source for intervertebral disc regeneration that is easier to obtain, has lower donorsite morbidity, and is available in larger numbers than stem cells harvested using bone marrow aspiration (Strong et al., 2012). Generally, in vitro NP-like differentiation of ASCs can hardly be achieved. Research reported that the combination of TGF- β 1 and the growth differentiation factor 5 can synergistically drive the NP-like differentiation process (Colombier et al., 2016). However, many issues still need to be considered, such as whether during induction of NP-like in vitro, cells adopt natural differentiation stages, and whether they can form ectopic stable NP-like tissue that is resistant to pathological changes in vivo.

Previously, we reported that GelMA hydrogel can protect cartilage from deterioration by promoting the accumulation of cartilage extracellular matrix (Chen et al., 2016). In this study, we used an optimised hydrogel to facilitate the ASCs' NP-like differentiation by supplying an appropriate micro-environment. For IVDD, many surgical treatments involving autologous BMSC implantation have been successfully used in animal studies (Longo et al., 2012; Wang, Wu, & Wang, 2010). However, these therapeutic methods mainly focused on the supply of cells and ignored the possibilities of osteogenic or adipogenic of the stem cells. In our study, we developed a strategy of combination

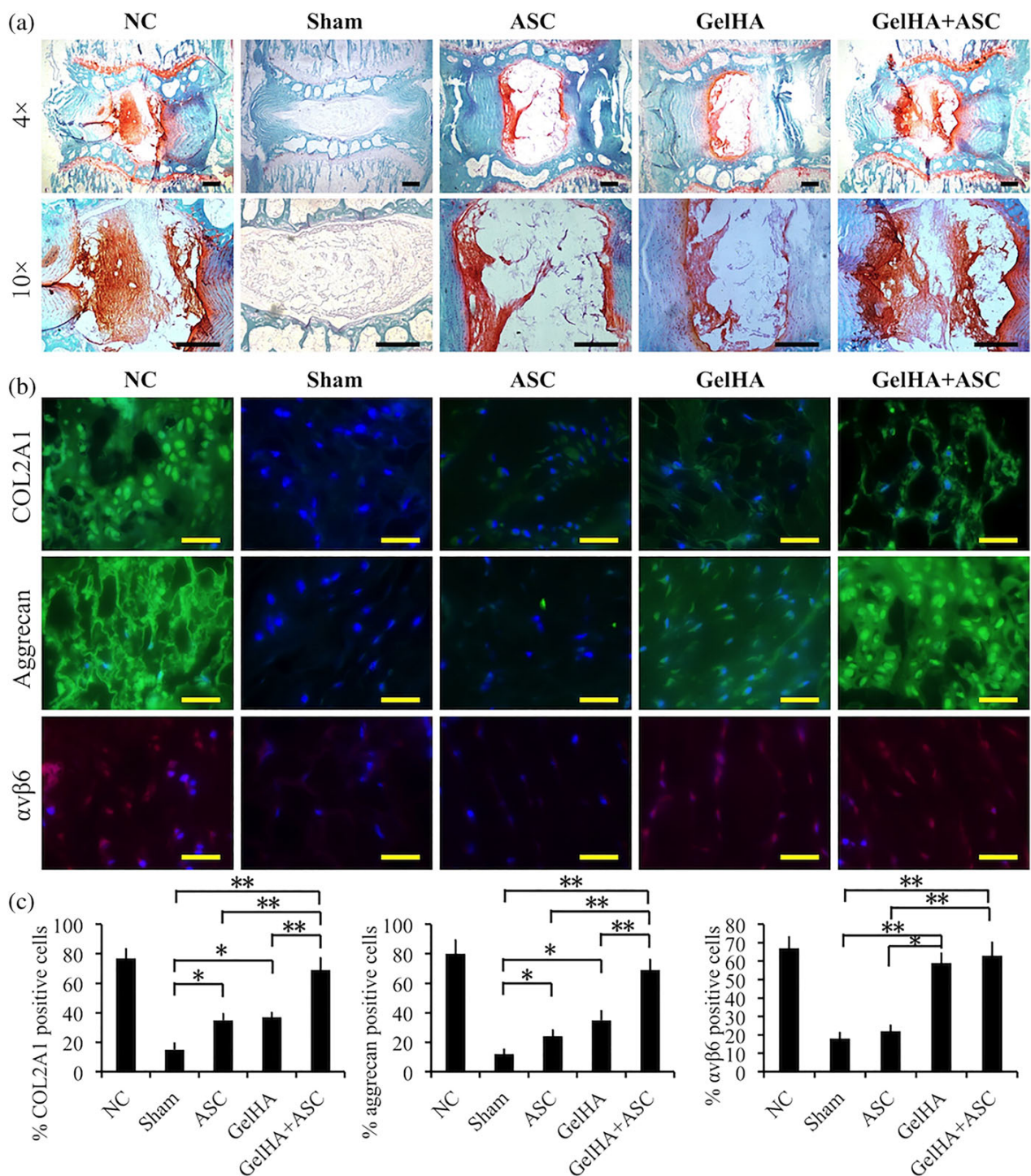


FIGURE 6 Effect of gelatin-hyaluronic acid methacrylate (GelHA)- adipose stromal cells (ASCs) on nucleus pulposus related matrix in vivo. (a) Safranin O staining of different groups at 12 weeks, scale bars = 200 μm. (b) Immunohistochemistry of MMP13, COL2A1, aggrecan, and integrin αvβ6 (12 weeks), Scale bars = 100 μm. (c) Quantification of COL2A1-positive, aggrecan-positive, and integrin αvβ6-positive-cells. n = 12 (biological replicates), **p* < 0.05, ***p* < 0.01 (one way analysis of variance) [Colour figure can be viewed at wileyonlinelibrary.com]

GelHA hydrogel and the ASCs to commit the NP-like differentiation of ASCs for IVDD repair. The results demonstrated that GelHA + ASCs have advantages over ASCs or GelHA alone in the treatment of IVDD

and disc height restoration in rat model. In this study, the regeneration of NP tissue included two aspects. At the initial time of implantation, GelHA hydrogel promoted the differentiation of ASCs into NP-like

cells. Then, the GelHA hydrogel gradually degraded and was replaced by the ECM produced by the NP-like cells. These processes guaranteed effective therapeutic IVD repair.

Previous studies have shown that GelMA hydrogels have the character of adhesion domains (Nichol et al., 2010), thermosensitivity (Van den Bulcke et al., 2000), and enzymatic degradability (Benton, DeForest, Vivekanandan, & Anseth, 2009), and support the formation of new ECM (Levett et al., 2014). In this study, GelHA hydrogels showed satisfying mechanical properties; these findings are consistent with previous studies that appropriate mechanical properties can be achieved by adjusting the components of the hydrogels (Camci-Unal et al., 2013). Also, in this study, we found by constructing an NP-like microenvironment, the integrin $\alpha\beta_6$ -TGF- β_1 pathway was activated. Hence, GelHA hydrogel might exert a certain therapeutic effect in IVDD treatment. There are also some limitations in this study. For example, UV irradiation may have a negative effect upon cell's DNA. In the future, we will focus on investigating a hydrogel with suitable mechanical strength, by using shorter-duration UV irradiation or visible light cross-linking.

5 | CONCLUSION

In this study, we have shown that the combination of photocrosslinked GelHA hydrogel and ASCs can commit ASCs to NP-like differentiation and improve the efficacy of ASCs for intervertebral disc repair by activating the integrin $\alpha\beta_6$ -TGF- β_1 pathway.

ACKNOWLEDGEMENTS

The study is sponsored by National Nature Science Fund of China [grant numbers 81802147, 81702143, 81772387, 81871797]; the Natural Science Fund of Zhejiang Province [grant numbers Y18H060001, LZ15H060002, LY16H060004]; and the Key research and development plan in Zhejiang Province [grant numbers 2018C03060].

CONFLICTS OF INTEREST

The authors have no conflicts of interest to declare.

ORCID

Shunwu Fan  <https://orcid.org/0000-0003-3443-4395>

REFERENCES

- Anderson, D. G., Albert, T. J., Fraser, J. K., Risbud, M., Wuisman, P., Meisel, H. J., ... Vaccaro, A. R. (2005). Cellular therapy for disc degeneration. *Spine (Phila Pa 1976)*, *30*(17 Suppl), S14–S19. <https://doi.org/10.1097/01.brs.0000175174.50235.ba>
- Baffi, M. O., Moran, M. A., & Serra, R. (2006). Tgfr2 regulates the maintenance of boundaries in the axial skeleton. *Developmental Biology*, *296*(2), 363–374. <https://doi.org/10.1016/j.ydbio.2006.06.002>
- Baffi, M. O., Slattery, E., Sohn, P., Moses, H. L., Chytil, A., & Serra, R. (2004). Conditional deletion of the TGF-beta type II receptor in Col2a expressing cells results in defects in the axial skeleton without alterations in chondrocyte differentiation or embryonic development of long bones. *Developmental Biology*, *276*(1), 124–142. <https://doi.org/10.1016/j.ydbio.2004.08.027>
- Benton, J. A., DeForest, C. A., Vivekanandan, V., & Anseth, K. S. (2009). Photocrosslinking of gelatin macromers to synthesize porous hydrogels that promote valvular interstitial cell function. *Tissue Engineering Part A*, *15*(11), 3221–3230. <https://doi.org/10.1089/ten.tea.2008.0545>
- Burdick, J. A., Chung, C., Jia, X., Randolph, M. A., & Langer, R. (2005). Controlled degradation and mechanical behavior of photopolymerized hyaluronic acid networks. *Biomacromolecules*, *6*(1), 386–391. <https://doi.org/10.1021/bm049508a>
- Camci-Unal, G., Cuttica, D., Annabi, N., Demarchi, D., & Khademhosseini, A. (2013). Synthesis and characterization of hybrid hyaluronic acid-gelatin hydrogels. *Biomacromolecules*, *14*(4), 1085–1092. <https://doi.org/10.1021/bm3019856>
- Carlesso, L. C., Raja Rampersaud, Y., & Davis, A. M. (2017). Clinical classes of injured workers with chronic low back pain: A latent class analysis with relationship to working status. *European Spine Journal*, *27*, 117–124. <https://doi.org/10.1007/s00586-017-4966-1>
- Chaofeng, W., Chao, Z., Deli, W., Jianhong, W., Yan, Z., Cheng, X., ... Dike, R. (2013). Nucleus pulposus cells expressing hBMP7 can prevent the degeneration of allogenic IVD in a canine transplantation model. *Journal of Orthopaedic Research*, *31*(9), 1366–1373. <https://doi.org/10.1002/jor.22369>
- Chen, P., Xia, C., Mei, S., Wang, J., Shan, Z., Lin, X., & Fan, S. (2016). Intra-articular delivery of sinomenium encapsulated by chitosan microspheres and photo-crosslinked GelMA hydrogel ameliorates osteoarthritis by effectively regulating autophagy. *Biomaterials*, *81*, 1–13. <https://doi.org/10.1016/j.biomaterials.2015.12.006>
- Clarke, L. E., McConnell, J. C., Sherratt, M. J., Derby, B., Richardson, S. M., & Hoyland, J. A. (2014). Growth differentiation factor 6 and transforming growth factor-beta differentially mediate mesenchymal stem cell differentiation, composition, and micromechanical properties of nucleus pulposus constructs. *Arthritis Research & Therapy*, *16*(2), R67. <https://doi.org/10.1186/ar4505>
- Colombier, P., Clouet, J., Boyer, C., Ruel, M., Bonin, G., Lesoeur, J., ... Guicheux, J. (2016). TGF-beta1 and GDF5 act synergistically to drive the differentiation of human adipose stromal cells toward nucleus pulposus-like cells. *Stem Cells*, *34*(3), 653–667. <https://doi.org/10.1002/stem.2249>
- Colombier, P., Clouet, J., Hamel, O., Lescaudron, L., & Guicheux, J. (2014). The lumbar intervertebral disc: From embryonic development to degeneration. *Joint, Bone, Spine*, *81*(2), 125–129. <https://doi.org/10.1016/j.jbspin.2013.07.012>
- Dong, X., Zhao, B., Iacob, R. E., Zhu, J., Koksai, A. C., Lu, C., ... Springer, T. A. (2017). Force interacts with macromolecular structure in activation of TGF-beta. *Nature*, *542*(7639), 55–59. <https://doi.org/10.1038/nature21035>
- Downing, T. L., Soto, J., Morez, C., Houssin, T., Fritz, A., Yuan, F., ... Li, S. (2013). Biophysical regulation of epigenetic state and cell reprogramming. *Nature Materials*, *12*(12), 1154–1162. <https://doi.org/10.1038/nmat3777>
- Levett, P. A., Melchels, F. P. W., Schrobback, K., Huttmacher, D. W., Malda, J., & Klein, T. J. (2014). A biomimetic extracellular matrix for cartilage tissue engineering centered on photocurable gelatin, hyaluronic acid and chondroitin sulfate. *Acta Biomaterialia*, *10*(1), 214–223. <https://doi.org/10.1016/j.actbio.2013.10.005>
- Longo, U. G., Papapietro, N., Petrillo, S., Franceschetti, E., Maffulli, N., & Denaro, V. (2012). Mesenchymal stem cell for prevention and management of intervertebral disc degeneration. *Stem Cells International*, *2012*, 921053. <https://doi.org/10.1155/2012/921053-921057>

- May, M. (2013). Regenerative medicine: Rebuilding the backbone. *Nature*, 503(7475), S7–S9. <https://doi.org/10.1038/503S7a>
- Minogue, B. M., Richardson, S. M., Zeef, L. A., Freemont, A. J., & Hoyland, J. A. (2010). Characterization of the human nucleus pulposus cell phenotype and evaluation of novel marker gene expression to define adult stem cell differentiation. *Arthritis and Rheumatism*, 62(12), 3695–3705. <https://doi.org/10.1002/art.27710>
- Nichol, J. W., Koshy, S. T., Bae, H., Hwang, C. M., Yamanlar, S., & Khademhosseini, A. (2010). Cell-laden microengineered gelatin methacrylate hydrogels. *Biomaterials*, 31(21), 5536–5544. <https://doi.org/10.1016/j.biomaterials.2010.03.064>
- Patrick, N., Emanski, E., & Knaub, M. A. (2014). Acute and chronic low back pain. *The Medical Clinics of North America*, 98(4), 777–789. xii. <https://doi.org/10.1016/j.mcna.2014.03.005>
- Steck, E., Bertram, H., Abel, R., Chen, B., Winter, A., & Richter, W. (2005). Induction of intervertebral disc-like cells from adult mesenchymal stem cells. *Stem Cells*, 23(3), 403–411. <https://doi.org/10.1634/stemcells.2004-0107>
- Strong, A. L., Semon, J. A., Strong, T. A., Santoke, T. T., Zhang, S., McFerrin, H. E., ... Bunnell, B. A. (2012). Obesity-associated dysregulation of calpastatin and MMP-15 in adipose-derived stromal cells results in their enhanced invasion. *Stem Cells*, 30(12), 2774–2783. <https://doi.org/10.1002/stem.1229>
- Vadala, G., Sowa, G., Hubert, M., Gilbertson, L. G., Denaro, V., & Kang, J. D. (2012). Mesenchymal stem cells injection in degenerated intervertebral disc: Cell leakage may induce osteophyte formation. *Journal of Tissue Engineering and Regenerative Medicine*, 6(5), 348–355. <https://doi.org/10.1002/term.433>
- Van den Bulcke, A. I., Bogdanov, B., De Rooze, N., Schacht, E. H., Cornelissen, M., & Berghmans, H. (2000). Structural and rheological properties of methacrylamide modified gelatin hydrogels. *Biomacromolecules*, 1(1), 31–38. <https://doi.org/10.1021/bm990017d>
- Wang, Y. T., Wu, X. T., & Wang, F. (2010). Regeneration potential and mechanism of bone marrow mesenchymal stem cell transplantation for treating intervertebral disc degeneration. *Journal of Orthopaedic Science*, 15(6), 707–719. <https://doi.org/10.1007/s00776-010-1536-3>
- Yang, X., & Li, X. (2009). Nucleus pulposus tissue engineering: A brief review. *European Spine Journal*, 18(11), 1564–1572. <https://doi.org/10.1007/s00586-009-1092-8>
- Ye, F., Lagarrigue, F., & Ginsberg, M. H. (2014). SnapShot: Talin and the modular nature of the integrin adhesome. *Cell*, 156(6), 1340–1340.e1341. <https://doi.org/10.1016/j.cell.2014.02.048-1340.e1>
- Zeng, Y., Chen, C., Liu, W., Fu, Q., Han, Z., Li, Y., ... Du, Y. (2015). Injectable microcryogels reinforced alginate encapsulation of mesenchymal stromal cells for leak-proof delivery and alleviation of canine disc degeneration. *Biomaterials*, 59, 53–65. <https://doi.org/10.1016/j.biomaterials.2015.04.029>
- Zhu, S., Chen, P., Wu, Y., Xiong, S., Sun, H., Xia, Q., ... Ouyang, H. W. (2014). Programmed application of transforming growth factor β 3 and Rac1 inhibitor NSC23766 committed hyaline cartilage differentiation of adipose-derived stem cells for osteochondral defect repair. *Stem Cells Translational Medicine*, 3(10), 1242–1251. <https://doi.org/10.5966/sctm.2014-0042>

SUPPORTING INFORMATION

Additional supporting information may be found online in the Supporting Information section at the end of the article.

Figure S1: 1H-NMR spectra of gelatin, hyaluronic acid and their methacrylamide forms. (a) 1H-NMR spectra of gelatin (left) and GelMA (right). The peaks in GelMA between 5 and 6 ppm shows the methacrylation of gelatin. (b) 1H NMR spectra of hyaluronic acid (left) and HAMA (right). The peaks between 1.5–2 ppm represents the methacrylation of hyaluronic acid.

Figure S2: Mechanical characterisation of GelHA hydrogels at different concentrations. The compressive moduli for hybrid hydrogels are found to be mechanically tunable. $n = 5$ (biological replicates), $*p < 0.05$, $**p < 0.01$ (one way ANOVA).

Figure S3: Negative control of integrin $\alpha\beta$ 6 immunostaining, scale bars = 100 μ m.

Figure S4: Diagram illustrating the proposed mechanism of action of integrin $\alpha\beta$ 6-TGF- β pathway in intervertebral disc.

How to cite this article: Chen P, Ning L, Qiu P, et al. Photocrosslinked gelatin-hyaluronic acid methacrylate hydrogel-committed nucleus pulposus-like differentiation of adipose stromal cells for intervertebral disc repair. *J Tissue Eng Regen Med*. 2019;13:682–693. <https://doi.org/10.1002/term.2841>